

Could two-dimensional perovskites fundamentally solve the instability of perovskite photovoltaics

Luoran Chen(陈烙然), Hu Wang(王虎), and Yuchuan Shao(邵宇川)

Citation: Chin. Phys. B, 2022, 31 (**11**): 117803. DOI: 10.1088/1674-1056/ac693e

What follows is a list of articles you may be interested in

A novel natural surface-enhanced fluorescence system based on reed leaf as substrate for crystal violet trace detection

Hui-Ju Cao(曹会菊), Hong-Wen Cao(曹红文), Yue Li(李月), Zhen Sun(孙祯), Yun-Fan Yang(杨云帆), Ti-Feng Jiao(焦体峰), and Ming-Li Wang(王明利)

Chin. Phys. B, 2022, 31 (**10**): 107801. DOI: 10.1088/1674-1056/ac7215

First principles investigation on Li or Sn codoped hexagonal tungsten bronzes as the near-infrared shielding material

Bo-Shen Zhou(周博深), Hao-Ran Gao(高浩然), Yu-Chen Liu(刘雨辰), Zi-Mu Li(李子木),Yang-Yang Huang(黄阳阳), Fu-Chun Liu(刘福春), and Xiao-Chun Wang(王晓春)

Chin. Phys. B, 2022, 31 (**5**): 057804. DOI: 10.1088/1674-1056/ac598a

A flexible ultra-broadband metamaterial absorber working on whole K-bands with polarization-insensitive and wide-angle stability

Tao Wang(汪涛), He-He He(何贺贺), Meng-Di Ding(丁梦迪), Jian-Bo Mao(毛剑波), Ren Sun(孙韧), and Lei Sheng(盛磊)

Chin. Phys. B, 2022, 31 (**3**): 037804. DOI: 10.1088/1674-1056/ac306e

Enhancing the photo-luminescence stability of $CH_3NH_3PbI_3$ film with ionic liquids

Weifeng Ma(马威峰), Chunjie Ding(丁春杰), Nasrullah Wazir, Xianshuang Wang(王宪双), Denan Kong(孔德男), An Li(李安), Bingsuo Zou(邹炳锁), and Ruibin Liu(刘瑞斌)

Chin. Phys. B, 2022, 31 (**3**): 037802. DOI: 10.1088/1674-1056/ac3067

Linear and nonlinear optical response of g-C_3N_4-based quantum dots

Jing-Zhi Zhang(张竞之) and Hong Zhang(张红)

Chin. Phys. B, 2021, 30 (**7**): 077802. DOI: 10.1088/1674-1056/abec2f

---

TOPICAL REVIEW — Emerging photovoltaic materials and devices

Could two-dimensional perovskites fundamentally solve the instability of perovskite photovoltaics

Luoran Chen(陈烙然)[1,2,3], Hu Wang(王虎)[1,3,†], and Yuchuan Shao(邵宇川)[1,2,3,4,‡]

[1] *Laboratory of Thin Film Optics, Shanghai Institute of Optics and Fine Mechanics, Chinese Academy of Sciences, Shanghai* 201800, *China*
[2] *Center of Materials Science and Optoelectronics Engineering, University of Chinese Academy of Sciences, Beijing* 100049, *China*
[3] *Key Laboratory of Materials for High Power Laser, Chinese Academy of Sciences, Shanghai* 201800, *China*
[4] *Hangzhou Institute for Advanced Study, University of Chinese Academy of Sciences, Hangzhou* 310024, *China*

(Received 19 November 2021; revised manuscript received 11 April 2022; accepted manuscript online 22 April 2022)

The high efficiency and low production cost enable the halide perovskite solar cells as a promising technology for the next generation photovoltaics. Nevertheless, the relatively poor stability of the organic–inorganic halide perovskites hinders their commercial applications. In the past few years, two-dimensional (2D) perovskite has emerged as a more stable alternative to the three-dimensional (3D) counterparts and attracted intense research interests. Although many attempts and advances have been made, it is still ambiguous that whether the 2D perovskites could bring closure to the stability issue. To answer this essential question, a systematic study of the nature of 2D halide perovskites is necessary. Here, we focus on the stability investigations of 2D perovskites from different perspectives, especially light, heat, ion migration and strain. Several remaining challenges and opening problems are also discussed. With further material and device engineering, we believe that the 2D perovskites would promote perovskite solar cells to a promising future.

Keywords: halide perovskite solar cells, two-dimensional perovskites, stability

PACS: 78.56.−a, 78.66.Db, 78.66.Sq, 81.07.St **DOI:** 10.1088/1674-1056/ac693e

1. Introduction

The levelized cost of electricity (LCOE), describing the average cost per unit of electricity over the lifetime of an energy system, is a convenient metric for comparing different generating sources. In terms of a photovoltaic (PV) technology, three criteria, including cost, power conversion efficiency (PCE) and lifetime determine its LCOE. As a potential game-changer to the PV market, organic-inorganic halide perovskites (OIHP) present competition edge in both cost and PCE. The raw materials for perovskite are widely available and can be bought from suppliers with a reasonable price. The typical perovskite absorber is fabricated through the single crystal growth or polycrystalline film deposition processes, which is generally realized in the low-temperature precursor solution. The LCOE of perovskite solar panels is estimated to be just about 10–20 cents per Watt, which is competitive over the 30 cents per Watt for traditional silicon-based panels.[1,2]

Benefiting from their remarkable physical properties, such as strong light absorption,[3,4] long carrier diffusion length[5–7] and high tolerance to defects,[8,9] the PCE of perovskite solar cells increased rapidly from 3.8% to 25.5% over the past few years,[10–14] on par with those of commercially available solar cells. With considerable research efforts, the PCE of large-area (65.0 cm^2) modules reached 19.54%.[15] However, the degradation of OIHP solar cell under moisture ambient,[16,17] thermal stress,[18,19] light illumination[20,21] and voltage bias stimulus[22,23] leads to a relatively short device lifetime, which remains a huge obstacle to the practical applications. The environmental stress such as the moisture intrusion or light degradation has been mitigated by encapsulation technology, whereas the ion migration within the materials under the operation condition (heat or electric field) is still a mysterious challenge.

Emerging as the more stable photovoltaic materials, two-dimensional (2D) perovskites have been developed rapidly in the past few years, which yields a possible solution for the stability issue of three-dimensional (3D) perovskites.[24,25] The hydrophobic and structure properties of the organic spacer ligands provide a molecular encapsulation to prevent moisture intrusion. The first solar cell based on 2D perovskites showed 4.73% PCE and superior moisture stability.[24] Interestingly, the inorganic octahedral layer within the quasi-2D perovskites is oriented to the substrate through a special method, which facilitates the transport of light-generation charge carrier and improves the PCE dramatically.[26,27] Such a photovoltaic device based on phase-pure thin films with microscale vertically aligned grains had achieved 16.25% PCE.[28] Furthermore, the solar cells retained 93.8% original PCE after store under ambient conditions of $65 \pm 10\%$ relative humidity for 4680 hours. However, the published stability tests conducted

†Corresponding author. E-mail: wanghu@siom.ac.cn
‡Corresponding author. E-mail: shaoyuchuan@siom.ac.cn

© 2022 Chinese Physical Society and IOP Publishing Ltd

in non-standard conditions are still far away from the famous acceleration aging test in thin film photovoltaic industry, which requires 1000 hours operational lifetime under 85 °C and 85% relative humidity.[1]

In this review, we critically discuss one essential question: whether 2D perovskites could fundamentally solve the instability of perovskite photovoltaics. At first, we give a brief introduction on the structure of the typical 2D perovskites and discuss the preferred stability from the thermodynamic insight. Then we discuss various operating issues which affect the stability and lifetime of OIHPs. The advantage of the 2D perovskites on the operation stability is summarized and the remained opening problems are also given.

2. The 2D perovskites

2.1. Structure

The stable black phase of the traditional 3D halide perovskites generally takes a formular as ABX_3, in which the metal cation B^{2+} and halide anion X^- form a BX_6 octahedra unit. The A^+ cation locates at the interstitial site among the octahedra and supports the 3D framework of X-sharing octahedra, which plays a critical role in affecting the associated structure stability, as shown in Fig. 1(a). When incorporating a large enough A^+ cation that exceeding the tolerance limit of the ABX_3 structure, the 3D framework will be broken up into the lower dimensional structures along with significant surface recombination.

Conceptually, 2D perovskites arise from cutting 3D perovskites along the specific crystallographic plane, the inorganic BX_6 nanosheet in the form of corner-sharing metal halide octahedral and separated by the organic spacer layer. The category of the organic groups and the inorganic layer number n separated by the organic groups yield a flexible degree of freedom on structure and electronic properties. The typical 2D perovskites are usually categorized into Ruddlesden–Popper (RP)[29,30] and Dion–Jacobson (DJ).[31,32] The formula of RP and DJ phase is $R_2(A)_{n-1}B_nX_{3n+1}$ and $R'(A)_{n-1}B_nX_{3n+1}$, in which R and R′ is organic spacer cation with monamine and diamine, respectively, as shown in Fig. 1(b). One of the hydrogen atoms belonging to the amine forms a hydrogen bond with the nearest X atom. The layer number n in the formula can be understood as the thickness of the inorganic layer. In most cases of the PV applications, the quasi-2D perovskites with layer number n greater than one were selected to balance the stability and performance.

2.2. Thermodynamic stability

Due to the larger interstitial surrounded by the octahedra, the interaction between A^+ cation and octahedra is constituted by hydrogen bond and van der Walls (vdW). Taking $MAPbI_3$ as a typical OIHP material, the formation energy is calculated as the energy difference between $MAPbI_3$ and corresponding iodides. The more negative value indicates the better thermodynamic stability. The first-principles calculations reveal that the formation energy of $MAPbI_3$ is about −0.27 eV.[8] In Fig. 1(c), the thermodynamic stable range is narrow for the equilibrium growth of $MAPbI_3$, which indicates the synthesis process should be carefully controlled to obtain stoichiometric $MAPbI_3$ perovskite phase.

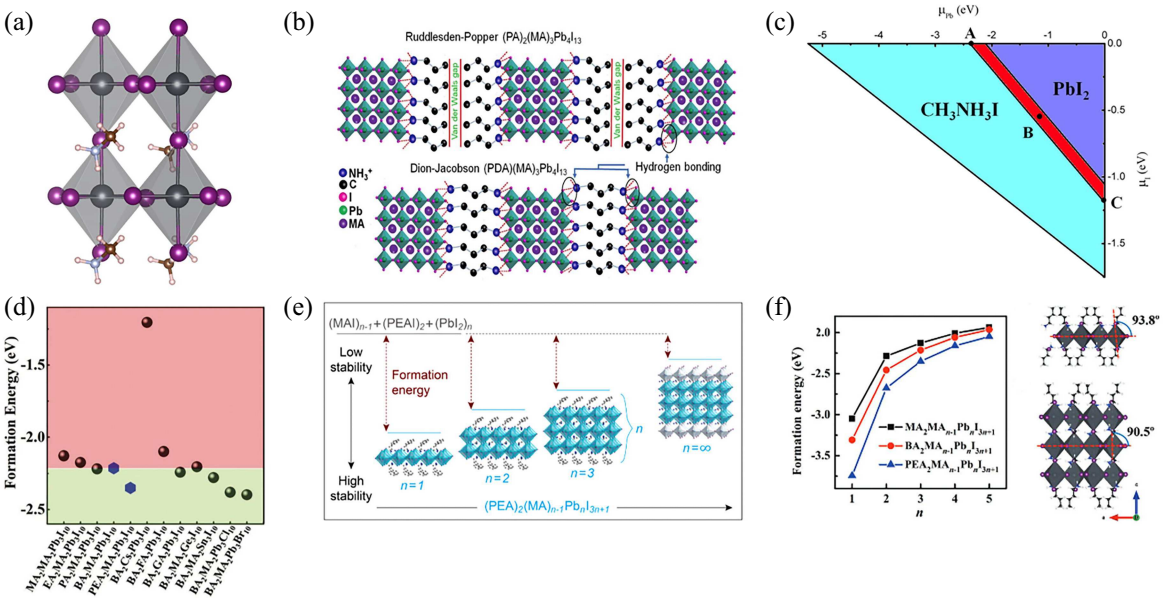


Fig. 1. Schematic illustration of (a) 3D and (b) RP or DJ phase 2D perovskites.[41] Reproduced with permission from Ref. [41]. (c) Thermodynamic stable range for equilibrium growth of $MAPbI_3$. Outside this region, the compound will decompose into PbI_2 and MAI.[8] Reproduced with permission from Ref. [8]. (d) Formation energy of 2D perovskites.[36] Reproduced with permission from Ref. [36]. (e) Relationship between stability and formation energy.[42] Reproduced with permission from Ref. [42]. (f) Formation energy as function of the thickness. Side view of orthorhombic and tetragonal BA_2PbI_4. The tilting angles are marked.[36] Reproduced with permission from Ref. [36].

The breakdown of the 3D framework due to the larger organic group in the 2D perovskites enables the extra relaxation or distortion of octahedra and reliefs the internal strain. Although the α-phase with Cs^+ or FA^+ cations is a high-temperature metastable phase, the surface energy of such metastable phase is often lower than that of the thermodynamically stable phase.[33] Therefore, perovskite phase of the 2D categories is much more stable due to the significant surface contribution. Especially, long-chain alkyl or aromatic ammonium cations are used to separate the BX_6 octahedral layer, which could further decrease the surface energy. With the decreasing of the number of the BX_6 nanosheet layers between the two layers of the organic chains, the surface contribution is far more dominant.[34] Both the experimental results and first-principles calculations[35] indicate that the formation energy of the 2D perovskite is much more negative than the 3D one ($n = \infty$), as shown in Fig. 1(d). Interesting, the hydrophobicity of the 2D perovskite is also significantly improved due to the lower surface energy. In addition, the dominant surface environment allows flexible distortion and relaxation of the octahedra, which is the main reason for the lower surface energy.[36] Comparing with the composition engineering, the phase purity and environmental stability of the 2D perovskites are usually more outstanding, and the processing conditions are more controllable. Nevertheless, the adjacent organic groups in the 2D RP perovskites are weakly interacted through the vdW force between the ammonium groups. Such a vdW force could be eliminated in the DJ phase since the diamine in the DJ phases can directly bridge the adjacent inorganic nanosheets with two hydrogen bonds. Therefore, the thermodynamic stability of the DJ phase is expected to be better than that of the RP phase.[37] The unencapsulated quasi-2D DJ perovskites were reported to sustain over 95% of its initial PCE after storage in N_2 for 1655 hours at 80 °C.[38] Although a better balance between photovoltaic efficiency and stability is expected to be realized on the 2D/3D mixture perovskites or layered 2D/3D perovskites,[39,40] the thermodynamic stability is really dominated by the surface functionalization of the 2D components, which yields a strong interlock between the stability and efficiency.

3. Stability under operation

Under direct sunlight, the temperature of perovskite materials inside the solar cell can reach above 70 °C, which increases the risk of thermal decomposition of the OIHPs.[43] The perovskite materials and the transport layers are also vulnerable to the sunlight and moisture. The ion migration driven by the inner electric field or strain is a far more intractable and fundamental problem that must be confronted for a feasible solution of perovskite photovoltaic. Firstly, the degradation originating from the moisture will be given briefly since it has been understood well both theoretically and experimentally. Next, we aim to give a detailed description on migration mechanism, characterization method and several remarking developments for the ion migration. Finally, several operation stresses related to ion migration are discussed. The advantages and certain opening questions on the 2D perovskites are elaborately listed in each subsection.

3.1. Moisture

The first-principles calculations reveal that the water absorption energy is as low as 0.30 eV and the water molecular can penetrate the inner inorganic layers through the framework of MA^+ easily.[44] In Fig. 2(a), the migration barrier of the water molecular through the MA^+ group is as low as 0.04 eV. When the MA^+ on the surface is replaced with BA^+, the migration barrier increases to 0.72 eV, as shown in Fig. 2(b). Shi *et al.* discussed the influence of various typical organic spacer ligands on the water migration barrier of quasi-2D perovskites.[36] From Fig. 2(c), we can find that the MA^+ shows the lowest migration barrier, whereas the others' migration barrier is at least 0.5 eV higher than that of the MA^+. The hydrophobic of the organic group in quasi-2D perovskites is beneficial to enhance the moisture stability of solar cell and protects the octahedral framework from the invasion of water molecular.[36,45] Generally, the grain boundary in the 3D polycrystalline film often orients randomly, as shown in Fig. 2(d). The primitive structure is combined by the vdW force between organic groups of quasi-2D perovskites, which increases the structure order and often shows a better crystal quality. Ren *et al*. applied a tailored organic ended with the sulfur (herein labeled as MTEA) to fabricate a quasi-2D RP phase perovskite, which enables a strong interaction between the sulfur atoms in addition to the weak vdW interaction.[46] Such a specific interlayer enhances the charge transport and stabilization, along with moisture tolerance for up to 1512 hours under 70% humidity. From Figs. 2(e)–2(h), the popular BA^+ group can sustain 840 hours before the appearance of the PbI_2 phase, whereas the 3D analog survives less than 120 hours.[47] In fact, the properties of the MTEA group would be much more similar with the DJ phase if the S–S interaction is much stronger. It is affirmative that the reported lifetime is more than 23 days for the DJ phase, as shown in Fig. 2(i).[38] The thorough study on the DJ phase layer perovskites in the future will greatly push forward the commercial application of OIHP due to their unique structure and properties.

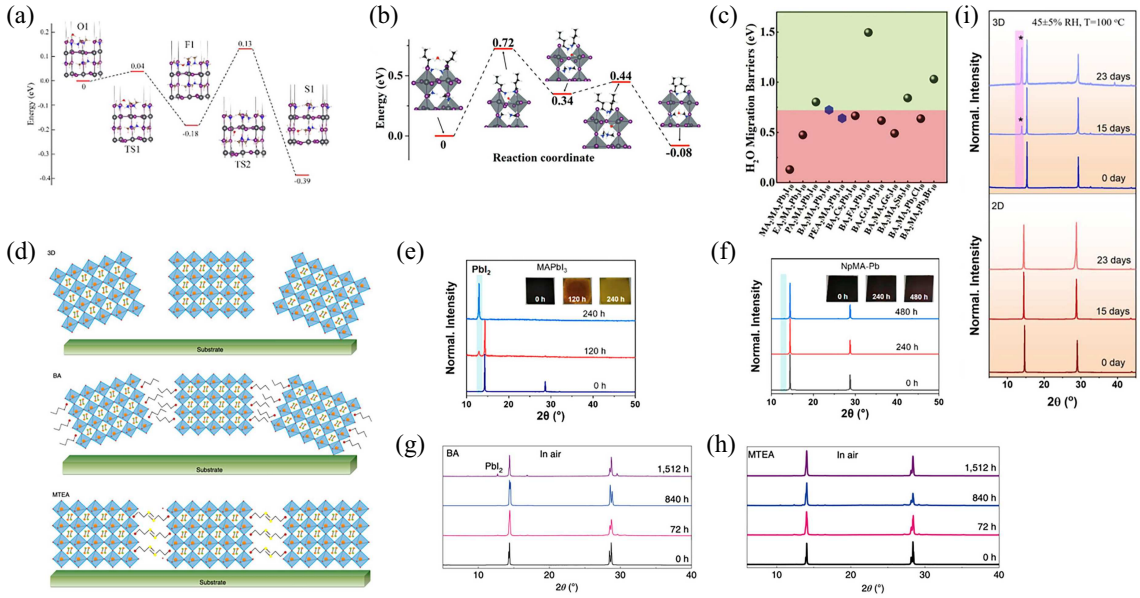


Fig. 2. Energy profile of different states during the penetration of water molecular through (a) MA^+[44] and (b) BA^+.[36] Reproduced with permission from Refs. [36,44], respectively. (c) Water molecular migration barrier of quasi-2D perovskites.[36] Reproduced with permission from Ref. [36]. Green/red background color is corresponding to favorable/unfavorable barrier as compared to the best experimental material. (d) Schematics from random orientation to vertical orientation of 3D, $(BA)_2(MA)_4Pb_5I_{16}$ and $(MTEA)_2(MA)_4Pb_5I_{16}$ perovskite films.[46] Reproduced with permission from Ref. [46]. XRD patterns of (e) $MAPbI_3$ and (f) NpMA-Pb films exposed in ambient air with an RH of 40%–50% for 0 hour, 240 hours, and 480 hours.[47] Reproduced with permission from Ref. [47]. Air stability of (g) $(BA)_2(MA)_4Pb_5I_{16}$ and (h) $(MTEA)_2(MA)_4Pb_5I_{16}$ perovskite films fabricated and tested in a room-temperature and 80% (±7%) relative humidity ambient atmosphere, completely without encapsulation.[46] Reproduced with permission from Ref. [46]. (i) XRD of 3D and 2D DJ perovskite films stored in air (RH = 45 ± 5%) at 100 °C.[38] Reproduced with permission from Ref. [38].

3.2. Ion migration

Ion migration driven by the electric field in perovskite absorbers has been generally recognized as one of the most detrimental pathways to degrade the OIHP devices. Due to the soft ionic bond and weak van der Waals interaction, the constituting ions (such as I^-, Pb^{2+}, MA^+) can easily escape from the lattice site and form various native point defects during the traditional process techniques. In addition, the surface and grain boundaries open another feasible pathway for the ion migration in the polycrystalline perovskite films.[48] It is reported that the photocurrent hysteresis is related with the ion migration and sensitive to the grain size and crystallinity of the 3D $MAPbI_3$.[22] Therefore, the ion migration is a more intrinsic problem that cannot be alleviated by encapsulation.

The ion migration in the solids is often realized by two steps: overcoming the bonding barrier of lattice site and occurrence of certain concentration vacancies or other open structures. Through the first-principles calculations of migration barrier for the preexistent defect, the vacancy and interstitial of I^- or MA^+ are revealed with high mobility. The calculated vacancy migration barrier is about 0.32 eV–0.45 eV for V_I and 0.57 eV–0.89 eV for V_{MA}.[49] As shown in Fig. 3(a), the migration barrier of V_I is similar with that of I_i, whereas the migration barrier of MA_i is much lower than that of V_{MA}.[50] Therefore, the V_I, I_i and MA_i could be the possible mobile ions in the $MAPbI_3$ perovskite.[51] The defect concentration dependent on the temperature can be evaluated via the formation energy, which is sensitive to the growth conditions. The formation energy of the typical intrinsic defects in Fig. 3(b) is listed as below:[8] $V_{MA} = 0.81$–2.01 eV, $V_{Pb} = 0.29$–2.68 eV, $V_I = 0.67$–1.87 eV; $I_i = 0.23$–1.42 eV, $MA_i = 0.20$–1.39 eV, $Pb_i = 1.85$–4.24 eV. The wide range of defect formation energy can be perceived with the distinct different observations on the experimental studies of ion migration. The deep level of the intrinsic defects is difficult to form due to significantly higher formation energy, which is the origin of the defect tolerance of perovskites.

Many researchers are aiming at finding out a direct evidence of ion migration in the $MAPbI_3$ perovskite. Temperature-dependent conductivity has always been a prevalent and achievable approach to characterize the activation energy of free carriers and different conductive mechanisms (in Fig. 4(a)), which is analyzed with the Nernst–Einstein equation.[48,52,53] The researchers tend to relate the activation energy at the higher temperature with ion migration.[54,55] Nevertheless, the halide perovskites have been recognized to be a mixed electronic–ionic character,[56–58] which hinders the direct analysis of ionic conductivity. Moreover, the mobility and diffusivity of the ions are far slower than that of the electrons or holes due to the large atomic mass and strong lattice bonding. Delicate and species-sensitive characterization method is required to confirm and quantify the details of ion migration.

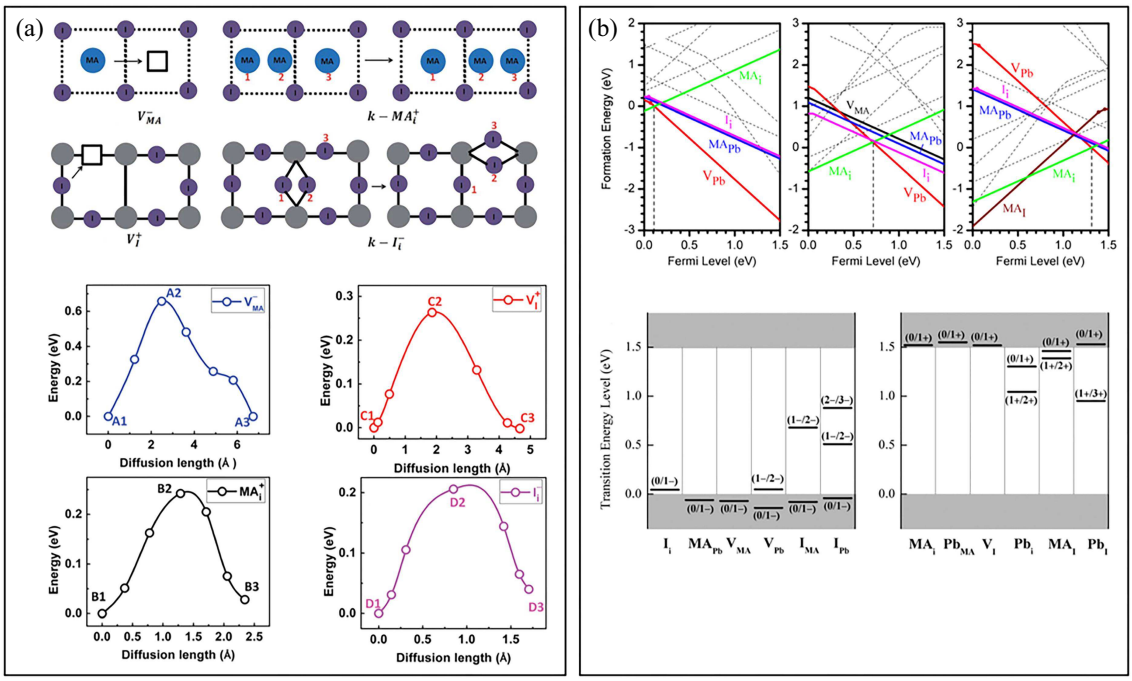


Fig. 3. (a) Schematic diagrams to show the diffusion paths through vacancies or interstitials as well as the corresponding migration energy profile.[50] Reproduced with permission from Ref. [50]. (b) The formation energies of intrinsic point defects in $MAPbI_3$ at chemical potentials A, B, and C shown in Fig. 1(c).[8] The corresponding transition energy level is also given. Reproduced with permission from Ref. [8].

Most first-principles calculations indicate that the iodine ions (vacancies or interstitials) are the most possible mobilizable species with the lowest migration energy.[49–51] The high mobility of iodine ions is qualitatively verified with the dynamic migrating of "PbI_2 thread"[59] along the electric field (in Fig. 4(b)) and the weight increase or formation of iodine-compounds at anode with the Tubandt method (in Fig. 4(c)).[56,58] The spectrometry method such as time-of-flight secondary ion mass spectrometry[60] (in Fig. 4(d)) or glow discharge optical emission spectroscopy[61] (in Fig. 4(e)) further confirms the migration of iodine ions under illumination or bias. Considering the sensitivity of bandgap on the mixed ratio of halides, the absorption and the emission spectra can directly monitor the halide ion diffusivity through the mixed halide perovskites.[62] In addition, the alternating-current (AC) impedance spectra is usually used to characterize the distinct ion-diffusion at low frequency and quantify the ion diffusivity.[57,58] Interestingly, the first experimentally verified migration specie is MA^+ vacancy rather than I^- vacancy, which is observed by the change of the Kelvin probe force microscopy (KPFM) potential images between two electrodes of $MAPbI_3$ thin film before and after 100 s electrical poling (Fig. 4(f)).[63] Due to the migration of MA^+ vacancy, the surface potential distribution of the $MAPbI_3$ film gradually increases from the region near the cathode (right) to the region near the anode (left), confirming the formation of a p–i–n junction near the cathode.

Plenty of evidences indicate that the perovskite-type halides exhibit a mixed conductive behavior including both the electronic conductivity and ionic conductivity, especially under the illumination.[56–58] A more accurate method is required to separate the ionic conductivity from the electronic conductivity. The ion transport property is often comprehended as the Warburg impedance in the low frequency region of the AC impedance spectra.[57] The electronic conductivity could be extracted as the high frequency limit from the AC impedance spectra at various temperature.[56,58] The temperature-dependent electronic conductivity shows an activation energy about 0.40 eV at the higher temperature,[58] which is similar with the value extracted from the conductivity curve without differentiating the specific conductivity mechanism.[48,52–55,63] The Tubandt method in Fig. 4(c) reveals that the halogen ion vacancies in the $MAPbI_3$ perovskite are highly mobile but limited by the vacancy concentration,[56,58] which indicates that both the electronic and ionic conductivities at the higher temperature are determined by the vacancy formation energy. Although the ion migration requires to overcome the migration barrier (~ 0.32 eV) of the preexistent defect, the actual barrier could be much lower due to the surface and grain boundaries inside the polycrystalline films or powders. Therefore, it is reasonable to observe similar activation energy for the electronic and ionic conductivities unless in a high-quality single crystal. The ion-blocking method is an efficient approach to extract the direct-current electronic and ionic conductivities respectively by analyzing the start voltage and the steady voltage with the electronic electrodes. The measurement on the $MAPbI_3$ powders shows $\sigma_e = 1.9 \times 10^{-9}$ S·cm^{-1} and $\sigma_i = 7.7 \times 10^{-9}$ S·cm^{-1}

at the dark condition.[58] The electronic conductivity is much more sensitive to the illumination conditions than the ionic conductivity. Nevertheless, the electronic and ionic conductivities could be significantly different in the actual samples due to the complex defect configurations under the operating and measuring conditions.

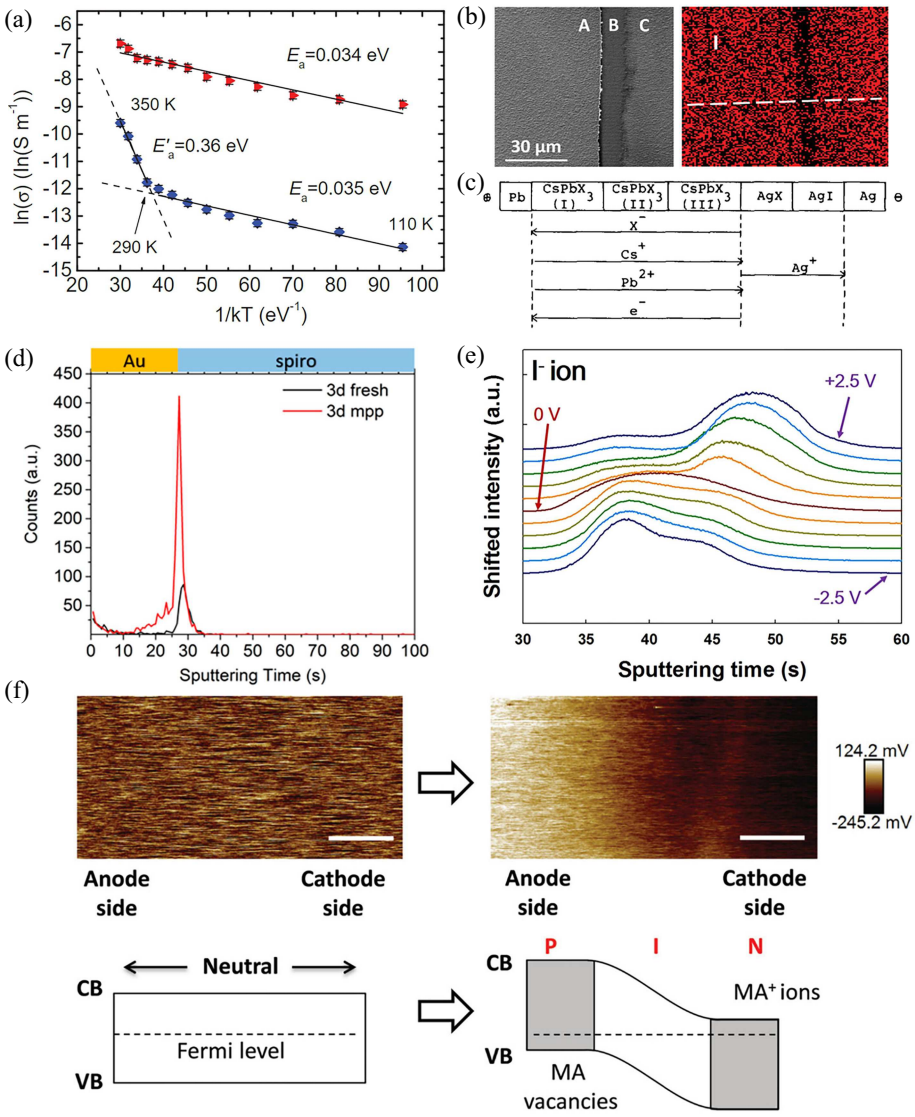


Fig. 4. (a) Arrhenius plot of the conductivity of the $MAPbI_3$ film under dark (blue) and illumination (red).[63] Reproduced with permission from Ref. [63]. (b) SEM image of a typical PbI_2 thread and corresponding concentration mapping of iodine element in a lateral device with a PbI_2 thread.[59] Reproduced with permission from Ref. [59]. (c) Flow directions of the charged species in cell with Tubandt method.[56] Reproduced with permission from Ref. [56]. I^- depth profile under (d) maximum power point (mpp) illumination[60] and (e) bias.[61] Reproduced with permission from Refs. [60,61], respectively. (f) KPFM potential images between two electrodes of $MAPbI_3$ thin film before and after 100 s electrical poling. The energy level diagrams of $MAPbI_3$ thin film before and after electrical poling are also given.[63] Reproduced with permission from Ref. [63].

As Yuan *et al.* suggested, the chemical structures of the traditional 3D perovskites would have to be modified if the bulk ion migration dominated under illumination.[48] In addition, large-size and high-quality single crystal is demanded for the traditional perovskites to eliminate the surface or grain boundaries. Recently, the development of 2D perovskites provides the extra freedoms to optimize the crystalline quality and defect modulation. An exciting result is reported that the ion migration is suppressed along both the in-plane and out-plane in the quasi-2D perovskite with BA^+-based RP structures (Fig. 5(a)),[54,55] even under the illumination conditions and up to 350 K. The ion migration along the out-plane is effectively prevented by the relative larger size of the long-chain organic ligands, while the diffusion along the in-plane is suppressed by the higher vacancy formation energy in the 2D perovskites. Nevertheless, it is difficult to determine the actual migration pathway and species through the conductivity measurement. The depth profile of Au_2I^- using the TOF-SIMS clearly illustrates the suppression of I^- immigration through the quasi-2D perovskite ($n = 40$) operating at the maximum power point.[60] As shown in Fig. 5(b), Cho *et al.* tracked the temperature-dependent absorption and emission spectra to monitor halide compositional variation during the ion migration in 2D perovskites with various layer numbers (n = 1–

10).[62] The activation energy characterizing the halide ion mobility decreases rapidly with the decrease of the layer number, which provides a direct evidence for the suppression of halide ion migration in 2D perovskites. First-principles calculation indicates that the elimination of organic molecules (i.e., BA^+, PEA^+) requires more energy than the MA^+ and the formation energy of the same defect in the 2D perovskites is much higher than that in the 3D counterparts.[64] The 2D perovskite (PEA_2PbI_4) is also applied at the grain boundaries of the 3D perovskites to suppress the ion migration and stabilize the perovskite phase of the matrix, which enhances the device stability with less than 1% relative efficiency loss in over 80 hours. More results have been reported to improve the device lifetime with the addition of 2D perovskites to passivate the grain boundaries. As mentioned in the above section, the normally metastable perovskite phase in the room temperature is more stable in the 2D perovskites due to significant surface contribution and structure relaxation as the decrease of the layer number. Therefore, the crystalline quality of 2D perovskites is often better controlled under the usually processing conditions than that of the traditional perovskites. In summary, the development of the 2D perovskites is a promising solution to resolve the intrinsic instability of the OIHP solar cells.

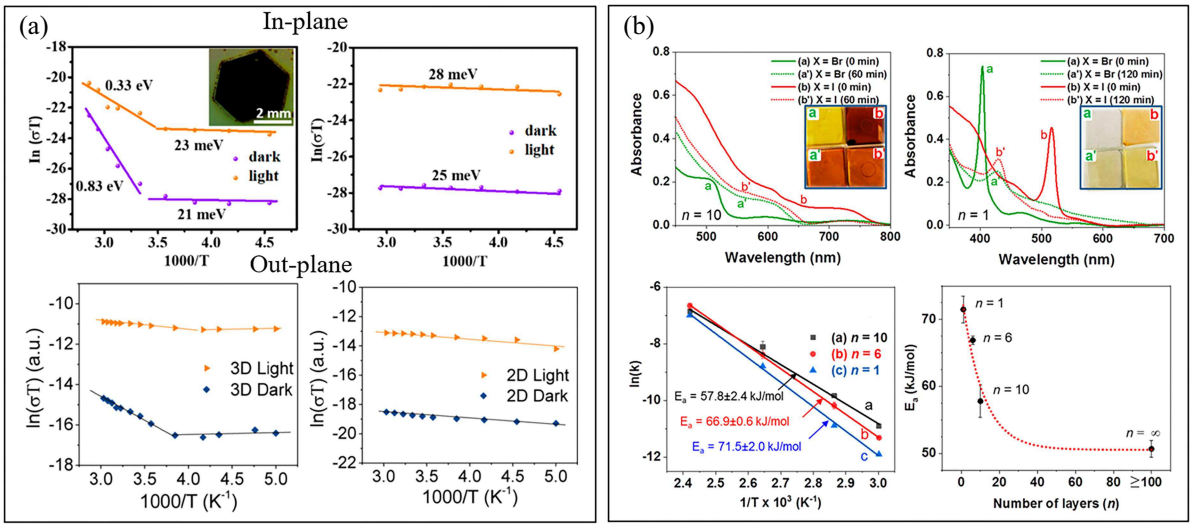


Fig. 5. (a) Temperature dependent conductivity measurement of 3D and 2D perovskite single crystals for in-plane.[55] Reproduced with permission from Ref. [55]. Temperature dependent conductivity measurement of 3D and 2D perovskite polycrystalline films for out-plane.[54] Reproduced with permission from Ref. [54]. (b) Absorption spectra of the two separated 2D lead halide (X = Br and I) perovskite films with different layers of $n = 10$ and $n = 1$ before and after homogenization at 140 °C. Arrhenius plots of $\ln(k)$ versus $1/T$ obtained from the 2D lead halide perovskite films with different layers. Activation energy versus number of layers.[62] Reproduced with permission from Ref. [62].

3.3. Thermal decomposition

In contrast with the traditional semiconductors used in the photovoltaics, the degradation temperature of the OIHPs (in particular $MAPbI_3$) is excessive low. Under direct sunlight, the temperature of perovskite materials can reach above 70 °C, which could lead to the phase transition and thermal decomposition of the OIHPs.

For a thermodynamically open system, the $MAPbI_3$ is facilely degraded into the PbI_2 yellow reactants and volatile components such as MAI at a rather low operation temperature within the solar cell.[43] The ionic bonding between A^+ and I^- is weakened when A^+ is an organic cation. Composition engineering generally uses the mixed cations or halides to stabilize the desired high-temperature perovskite phase at the operation temperature and achieve a balance between perovskite phase and thermal stability.[65] Lee *et al.* replaced 10% of FA^+ with the Cs^+ in $FAPbI_3$ perovskite and substantially improved stability along with photovoltaic performance.[66] The interaction between organic cation and octahedra is enhanced and the trap density is reduced. Jeon *et al.* demonstrated that mixing of MA^+ and FA^+ can stabilize the perovskite phase of $FAPbI_3$ and achieve more than 18% PCE under a standard illumination.[67] Saliba *et al.* showed that the "triple cation" ($Cs^+/MA^+/FA^+$) perovskite compositions are thermally more stable with the purer phase.[68] The resulting triple cation perovskite composition is less sensitive to processing conditions and reaches a stabilized power output of 21.1% and $\sim$ 18% after 250 hours under operational conditions. The optical density is stable when the sample is annealed at 130 °C for 3 hours in dry air. Most attention about composition engineering is concentrated on the improvement of the crystalline quality and intrinsic thermal stability, whereas the humidity issues are left with the encapsulation technology.

Decoupling of various environmental stress is one of the major difficulties on the study of thermal stability since the photodegradation and humidity are usually more detrimental than the thermal stress in the OIHP solar cells.[69] Therefore, the meaningful thermal stability experiments should be executed in the moisture-free and anaerobic setup under dark conditions. Moreover, the investigation of ion migration is always conducted under temperature-dependent conditions. Herein,

we shall concentrate on the thermal decomposition under the operation temperature (40–80 °C), which is more intrinsic and independent of the other environmental issues.

Although the repaid development of the advanced sealing techniques, the OIHP devices often show significant degradation after aging test with heat.[16] Conings *et al.* gave the first direct evidence that significant structural changes and decompositions already emerge within the $MAPbI_3$ perovskite even in the inert gas, while are further accelerated by the oxygen and humidity.[70] Even though the reported PCE maintains about 90% of the initial performance after 1000 hours under 60 ° in N_2 with the reasonable encapsulation,[71] the device is still far from the operation requirement for commercial application of solar cells . The thermal degradation process is characterized as the solid products PbI_2 and volatile components MAI. Thermal gravimetric and differential thermal analysis coupled with quadrupole mass spectrometry indicates that the MAI could further decompose into MA + HI or CH_3I + NH_3 pair gases under the heat stress.[69,72] The former is a reversible process that would be self-healed under the dark conditions if the device is well encapsulated as a close system. In contrast, the latter process is an irreversible process that would result in short lifetime of the $MAPbI_3$-based devices even if the system is isolated from the environment.[69] Such a degradation could be further accelerated if the absorber is exposed to the iodine vapor that is nearly inevitable during the sunlight or dark conditions during mild heating (40–80 °C).[73] Although the transformation between $MAPbI_3$ and PbI_2 is reported to be reversible, the recover reaction rate is much slower than the decomposition rate at the higher temperatures.[63] The above demonstrations suggest that the traditional $MAPbI_3$ perovskite may not be suitable for long-term stable solar cells and it is imperative to develop new structures of perovskite absorber to realize the commercialized OIHP devices.

The irreversible degradation pathway of the traditional perovskites demands careful selection of the stable organic cations at the A site. Fortunately, the perovskite layers are not homogeneously degraded, and the degradation paths usually nucleate at the free surface or grain boundary.[70] Abundant efforts are devoted to achieving large-size single crystal perovskites with uniform morphology and low density of defects or passivating the physical or chemical activated grain boundaries or surface.[3,67,71,74,75] For instance, the prepared perovskite solar cells maintain 90% of their initial efficiency of 21% after operation at the maximum power point under AM 1.5 G solar light at 60 °C for 1000 hours in N_2.[71] The recently developed 2D perovskites provide a versatile approach to encapsulate the BX_6 frameworks at the atomic or molecular scale with incorporating the larger organic cations (i.e., PEA, BA, AMP, PDA or ThDMA),[25,34,38,76] which could further decrease the surface energy. First-principles calculations of the desorption energy for the PEAI layer is about 0.36 eV greater than that of the MAI layer, which is independent of the number of layers in the slab.[42] The spacer organic cations in 2D perovskites are usually consisted of branched-chain, benzene, or phenol, which exhibits better hydrophobicity and higher desorption energy. The replacement of the more stable organic ligands at the surface or grain boundary suppresses the decomposition of MAI fundamentally as well as the irreversible reactive path. The surface energy of the metastable perovskite phase is often lower than that of the thermodynamically stable phase, which facilitates the high crystalline quality of the 2D perovskites.[33] Therefore, the reduce of grain density and the blocking of inorganic octahedron layer together could also suppress the migration of the detrimental species (such as iodine) and prolong the lifetime of the OIHP devices.

The improvement of thermal stability on the OIHP cells is rather impressive with the newly development 2D perovskites. Tsai *et al.* revealed that the quasi-2D RP phase $(BA)_2(MA)_{n-1}Pb_nI_{3n+1}$ series are more stable under heat stress of 80 °C than their 3D counterparts for the first time.[26] The degradation of the 3D perovskite thin film was observed by the emergency of the PbI_2 phase after 1 hour, whereas the $(BA)_2(MA)_3Pb_4I_{13}$ perovskite phase remained dominant in the 2D perovskites after 30 hours. As shown in Fig. 6(a), the DJ phase $(PDA)(MA)_3Pb_4I_{13}$ solar cell device retained about 95% PCE of the original value after 168 hours under harsh condition of 85 °C and 85% relative humidity, whereas the RP phase and 3D one decreased to almost 20% and 5% of the initial PCE, respectively.[41] Lu *et al.* achieved high efficient (> 15%) and thermal stable (maintaining 90% of the initial PCE after 350 hours at 80 °C) quasi-2D DJ perovskite with improved crystallinity, preferred vertical orientation and enlarged spatially resolved carrier lifetime.[38] The excellent thermal stability of the 2D perovskites is further applied to joint the grain boundaries within the 3D counterparts, which aims to achieve a better balance between photovoltaic efficiency and stability.[77,78]

3.4. Light stability

For photovoltaic applications that illuminated by sunlight for most of the daytime, light-induced degradation is a serious issue. To promote the commercialization of OIHP solar cell, the profound understanding of the light-induced degradation mechanism is necessary.[20,79–81] The light-induced degradation mechanism of conventional 3D perovskites is a complex dynamic process, accompanied by the photo-generated superoxide O_2^- to promote the deprotonation of methyl-ammonium as well as the migration of the halide ions. Recently, Anaya *et al.* clearly revealed that the electrostatic repulsion of the superoxide O_2^- negatively charge layer on the surface of OIHP created under illumination provides a driving force for halide ions to migrate toward bulk from illuminated areas, and the reaction between O_2^- anions and perovskite causes further degradation by formation of volatile methylamine.[82] Moreover, Hock *et al.* reported that phase segregation would occur in the mixed-halide hybrid perovskites after light-soaking

in the nitrogen environment. The light induced halide migration reduced the stability of the mixed-halide photovoltaic device.[83] In the field of silicon-based tandem solar cell, the material of top cell requires a bandgap of about 1.75 eV to achieve current-match both junctions,[84] which can be attained by using mixed halide perovskites. However, phase segregation caused by light-soaking is an intrinsic problem as discussed above, which limits the application of 3D perovskite materials. Different from 3D perovskite materials, 2D perovskites can realize the wide range of bandgap via applying different organic ligands and changing the number of inorganic layer, which holds great potential in silicon-based tandem solar cell.

The research interest in light induced degradation mechanism of 2D perovskites is growing at the same time. The early work of Mohite *et al.* revealed the preeminent photostability of the vertically orientation near single crystalline $(BA)_2(MA)_3Pb_4I_{13}$ unsealed device by hot-casting method. The device maintained 80% initial PCE after 200 hours under AM 1.5 G illumination and slowly degenerated to about 70% after 2250 hours, whereas the 3D $MAPbI_3$ retained less than 10% initial PCE under the same condition.[26] However, the mechanism behind light induced degradation of 2D perovskites is rarely reported. Fang *et al*. reported that laser induced degradation of 2D perovskites originates from the release of organic ligands and HI from the edge and surface of the sample, following the distortion of inorganic octahedron promotes the collapse of framework and leaves 3D PbI_2 alone as shown in Fig. 6(c).[85] The reports about $MAPbI_3$ have demonstrated that above band gap photoexcitation induced deformation relates to the changes of the Pb–I bond angles.[86] In 3D perovskites, only one type Pb–I bond can be identified. However, there are two types of Pb–I bonds in 2D perovskites due to the difference of the organic–inorganic stacking pattern, including the Pb–I bonds in the plane of the inorganic framework, as well as the dangling Pb–I bonds along the out-plane that I^- anions interact with organic ligands by hydrogen bond. The significantly longer dangling Pb–I bonds along the out-plane lead to the more vulnerable degradation along the *c* axis due to the lower interaction of covalent bonding.[85] The light induced degradation of 2D perovskites may relate to the intensity of the incident light and photon energy, the further research about one sun illumination degradation mechanism of 2D perovskites is needed. The DJ phase 2D perovskites eliminate van de Waals gap in RP phase via diamine organic ligands alternately forming hydrogen bonds with the inorganic layer, which is expected to be more robust under light illumination. Ahmad *et al.* reported that the DJ phase $(PDA)(MA)_3Pb_4I_{13}$ unencapsulated solar cell retained more than 95% initial PCE after 3000 hours continuous light soaking, under AM 1.5G illumination inside the glove box (Fig. 6(b)).[41] Moreover, the light stability of low dimensional DJ phase tin perovskites is also impressive.[87] The unencapsulated 4AMP-15 device with 10.25% PCE maintained about 77% initial PCE after 500 hours, testing under continuous 1-sun illumination in N_2 atmosphere at 40 °C.[88]

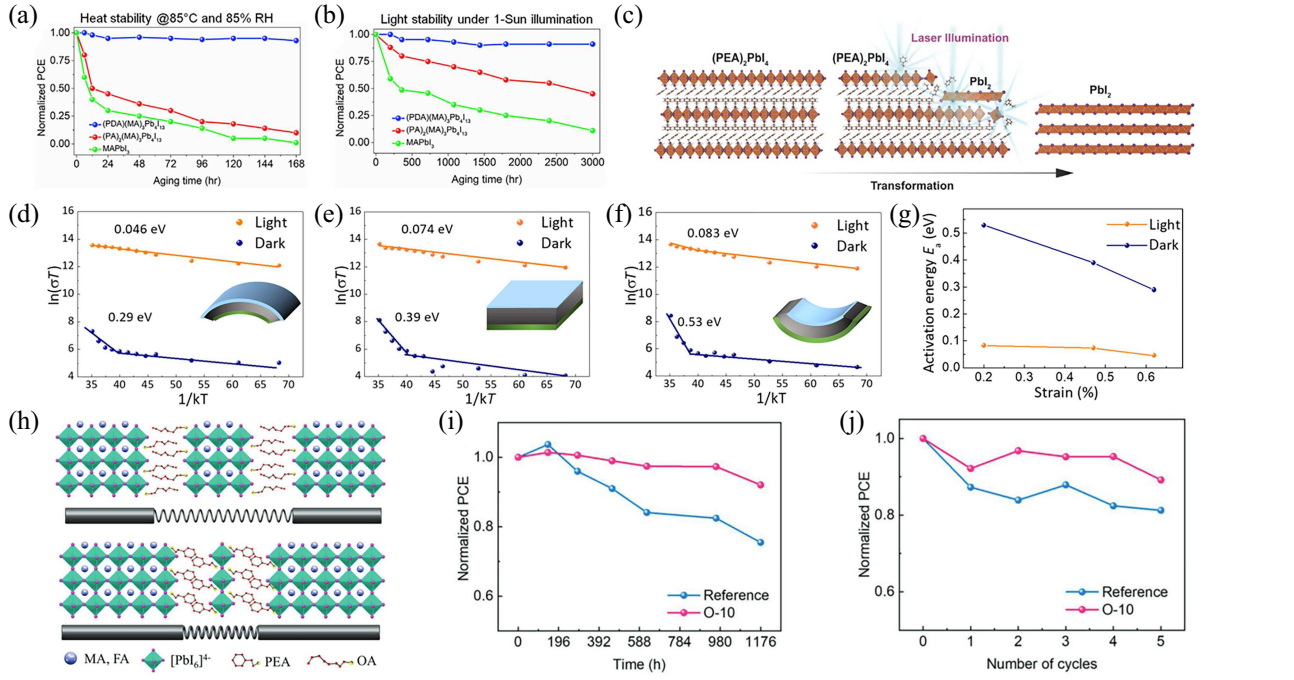


Fig. 6. Stability test of $MAPbI_3$, $(PA)_2(MA)_3Pb4I_{13}$, and $(PDA)(MA)_3Pb_4I_{13}$-based devices[41] under (a) damp heat stress (85 °C and 85% RH) and (b) light illumination. Reproduced with permission from Ref. [41]. (c) Schematic illustration of the structural evolution from $(PEA)_2PbI_4$ to PbI_2 under resonant excitation.[85] Reproduced with permission from Ref. [85]. The temperature-dependent conductivity[89] of the (d) convex film, (e) flat film and (f) concave film. (g) Variation of the activation energy of ion migration versus the strain in the $MAPbI_3$ films.[89] Reproduced with permission from Ref. [89]. (h) Schematic describing the residual stress relaxation with soft and stiff structural subunits.[93] (i) The long-term stability test of the perovskite solar cells stored in air with humidity 16%–50% for over 1000 h without encapsulation.[93] (j) Normalized devices' PCE after thermal stresses cycling between 85 °C and −40 °C arrangement.[93] Reproduced with permission from Ref. [93].

3.5. Strain stability

In addition to the typical degradation pathways discussed above, the lattice strain induce decomposition is another intrinsic instability of 3D halide perovskites. Such an issue was only studied by very few researchers and should attract enough attention from peers. Zhao *et al.* revealed that the mismatched thermal expansion between halide perovskites and substrate during the thermal annealing process leads to the compressive strain in the out-plane direction and the tensile strain in the in-plane. The lattice strain provides the additional driving force for the ion migration, accelerating the various degradation pathways in the former sections.[89] Lately, Wu *et al.* introduced a polystyrene between SnO_2 and perovskite as the buffer layer to release the residual stress during annealing.[90] The stress-free perovskite showed lower ion migration tendency and exhibited better device stability, which retained almost 97% of its initial PCE (21.89%) after 5 days of day–night loop. Moreover, Sargent's group reported that the compressive-strain (in-plane) perovskite by introducing a high thermal expansive coefficient hole-transport layer and elevating the processing temperature of hole-transport layer shows diminished ion migration to improve intrinsic stability.[91] Therefore, the photostability and thermal stability of compressive-strain perovskite are better than those of tensile-strain and non-strain ones.

The results of synchrotron x-ray powder diffraction and first principles calculation indicate that 2D perovskite $(BA)_2PbBr_4$ with lower Young's modulus is softer than most 3D perovskites.[92] The soft nature of 2D perovskites provides additional structural flexibility in terms of space to resist lattice distortion, thereby promoting stress relaxation. The stress relaxation mitigates the extra driving force for ion migration. In addition, stress relaxation also reduces the crystal imperfection that forms the paths of ion migration and therefore the overall stability is greatly improved. Wang *et al.* reported that two kinds of A-site cations octylammonium iodide (OAI) and phenethylammonium iodide (PEAI) incorporated into the surface of $FA_{0.85}MA_{0.15}Pb(I_{0.85}Br_{0.15})_3$ films could effectively release the surface residual stress.[93] The large organic cation OAI and PEAI treatment induced 2D perovskite component dwell at the surface of the perovskite thin film to construct soft structural subunits, providing more flexibility to reduce residual stress (Fig. 6(h)). The optimize device not only maintained 95% of the initial PCE (21.48%) after 1000 hours stored in air with 16%–50% humidity (Fig. 6(i)), but also retained about 90% initial PCE after 5 cycles thermal cycling test (Fig. 6(j)).

4. Conclusion and outlook

In this work, we have reviewed the major stability issues limiting the commercial application of organic–inorganic halide perovskites, as well as the prominent advantages of the 2D perovskites developed in the recent years. The structure and function of the 2D perovskites are much more feasible as the incorporation of large-size organic group between the $[BX_6]$ layer, which breaks down the 3D inorganic octahedral framework. Firstly, the notorious moisture and oxygen invasion is naturally shielded by the hydrophobicity of large-size organic group at the surface or grain boundary of 2D perovskites. The prerequisite encapsulation of the traditional perovskites can be ignored so that the device cost can be further decreased. Secondly, the suspension of the 3D framework due to the decorated organic group enables the extra freedom of twist and rearrangement for the $[BX_6]$ layer, which decreases the total energy of the perovskites and enhances the thermal stability intrinsically. Moreover, the $[BX_6]$ layer determining the excellent electronic properties is protected on the atomic or molecular scale, which is dependent on the number of the constituted $[BX_6]$ layers for one pair of organic groups. On the one hand, the atomic encapsulation of organic group in the 2D perovskites could prevent the leakage of volatile by-products and the reversible decomposition could be controlled or recovered during the environmental operation. On the other hand, the irreversible decomposition originated from the surface or grain boundary is dramatically suppressed due to the replacement for MA^+. Thirdly, the light-induced phase separation of 3D mixed-halide perovskites can be avoided in the 2D perovskites to apply in tandem solar cell since the bandgap can be modulated by the number of constituted layers. In addition, the degradation pathway due to the combination of light and oxygen is excluded with the isolation of oxygen by the organic group. However, the intrinsic decomposition pathway due to illumination is still not fully understood and needs more research efforts to clarify. Moreover, the soft nature of 2D perovskites provides additional flexibility to resist lattice distortion, thereby promoting stress relaxation. Finally, the suppression of ion migration has been revealed experimentally by various characterization methods for the 2D perovskites. Nevertheless, some results are still questionable due to the problem of separating the ion conductivity from the total conductivity. In summary, the development of the 2D perovskites seems to be a promising solution to resolve the intrinsic instability of the OIHP solar cells although several fundamental mechanisms such as light instability and ion migration require to be further solved.

Acknowledgement

Project supported by the National Natural Science Foundation of China (Grant Nos. 61805263 and 62104234).

References

[1] Meng L, You J B and Yang Y 2018 *Nat. Commun.* **9** 5265

[2] Song Z, McElvany C L, Phillips A B, Celik I, Krantz P W, Watthage S C, Liyanage G K, Apul D and Heben M J 2017 *Energy Environ. Sci.* **10** 1297

[3] Lee M M, Teuscher J, Miyasaka T, Murakami T N and Snaith H J 2012 *Science* **338** 643

[4] Yin W J, Shi T T and Yan Y F 2014 *Adv. Mater.* **26** 4653

[5] Stranks S D, Eperon G E, Grancini G, Menelaou C, Alcocer M J P, Leijtens T, Herz L M, Petrozza A and Snaith H J 2013 *Science* **342** 341

[6] Xing G C, Mathews N, Sun S Y, Lim S S, Lam Y M, Gratzel M, Mhaisalkar S and Sum T C 2013 *Science* **342** 344

[7] Dong Q F, Fang Y J, Shao Y C, Mulligan P, Qiu J, Cao L and Huang J S 2015 *Science* **347** 967

[8] Yin W J, Shi T T and Yan Y F 2014 *Appl. Phys. Lett.* **104** 063903

[9] Shi T T, Yin W J, Hong F, Zhu K and Yan Y F 2015 *Appl. Phys. Lett.* **106** 103902

[10] Kojima A, Teshima K, Shirai Y and Miyasaka T 2009 *J. Am. Chem. Soc.* **131** 6050

[11] Kim H S, Lee C R, Im J H, Lee K B, Moehl T, Marchioro A, Moon S J, Humphry-Baker R, Yum J H, Moser J E, Gratzel M and Park N G 2012 *Sci. Rep.* **2** 591

[12] Yang W S, Noh J H, Jeon N J, Kim Y C, Ryu S, Seo J and Seok S I 2015 *Science* **348** 1234

[13] Yang W S, Park B W, Jung E H, Jeon N J, Kim Y C, Lee D U, Shin S S, Seo J, Kim E K, Noh J H and Seok S I 2017 *Science* **356** 1376

[14] https://www.nrel.gov/pv/cell-efficiency.html

[15] Bu T, Li J, Li H, Tian C, Su J, Tong G, Ono L K, Wang C, Lin Z, Chai N, Zhang X L, Chang J, Lu J, Zhong J, Huang W, Qi Y, Cheng Y B and Huang F 2021 *Science* **372** 1327

[16] Han Y, Meyer S, Dkhissi Y, Weber K, Pringle J M, Bach U, Spiccia L and Cheng Y B 2015 *J. Mater. Chem. A* **3** 8139

[17] Yang J L, Siempelkamp B D, Liu D Y and Kelly T L 2015 *Acs Nano* **9** 1955

[18] Misra R K, Aharon S, Li B L, Mogilyansky D, Visoly-Fisher I, Etgar L and Katz E A 2015 *J. Phys. Chem. Lett.* **6** 326

[19] Divitini G, Cacovich S, Matteocci F, Cina L, Di Carlo A and Ducati C 2016 *Nat. Energy* **1** 15012

[20] Bryant D, Aristidou N, Pont S, Sanchez-Molina I, Chotchunangatchaval T, Wheeler S, Durrant J R and Haque S A 2016 *Energy Environ. Sci.* **9** 1655

[21] Yuan H F, Debroye E, Janssen K, Naiki H, Steuwe C, Lu G, Moris M, Orgiu E, Uji-i H, De Schryver F, Samori P, Hofkens J and Roeffaers M 2016 *J. Phys. Chem. Lett.* **7** 561

[22] Xiao Z G, Yuan Y B, Shao Y C, Wang Q, Dong Q F, Bi C, Sharma P, Gruverman A and Huang J S 2015 *Nat. Mater.* **14** 193

[23] Eames C, Frost J M, Barnes P R F, O'Regan B C, Walsh A and Islam M S 2015 *Nat. Commun.* **6** 7497

[24] Smith I C, Hoke E T, Solis-Ibarra D, McGehee M D and Karunadasa H I 2014 *Angew. Chem. Int. Ed.* **53** 11232

[25] Cao D H, Stoumpos C C, Farha O K, Hupp J T and Kanatzidis M G 2015 *J. Am. Chem. Soc.* **137** 7843

[26] Tsai H H, Nie W Y, Blancon J C, Toumpos C C S, Asadpour R, Harutyunyan B, Neukirch A J, Verduzco R, Crochet J J, Tretiak S, Pedesseau L, Even J, Alam M A, Gupta G, Lou J, Ajayan P M, Bedzyk M J, Kanatzidis M G and Mohite A D 2016 *Nature* **536** 312

[27] Zhang X Q, Wu G, Yang S D, Fu W F, Zhang Z Q, Chen C, Liu W Q, Yan J L, Yang W T and Chen H Z 2017 *Small* **13** 1700611

[28] Liang C, Gu H, Xia Y D, Wang Z, Liu X T, Xia J M, Zuo S W, Hu Y, Gao X Y, Hui W, Chao L F, Niu T T, Fang M, Lu H, Dong H, Yu H, Chen S, Ran X Q, Song L, Li B X, Zhang J, Peng Y, Shao G S, Wang J P, Chen Y H, Xing G C and Huang W 2020 *Nat. Energy* **6** 38

[29] Ruddlesden S N and Popper P 1957 *Acta Cryst.* **10** 538

[30] Ruddlesden S N and Popper P 1958 *Acta Cryst.* **11** 54

[31] Dion M, Ganne M and Tournoux M 1981 *Mater. Res. Bull.* **16** 1429

[32] Jacobson A J, Johnson J W and Lewandowski J T 1985 *Inorg. Chem.* **24** 3727

[33] Fu Y P, Wu T, Wang J, Zhai J Y, Shearer M J, Zhao Y Z, Hamers R J, Kan E J, Deng K M, Zhu X Y and Jin S 2017 *Nano Lett.* **17** 4405

[34] Stoumpos C C, Cao D H, Clark D J, Young J, Rondinelli J M, Jang J I, Hupp J T and Kanatzidis M G 2016 *Chem. Mater.* **28** 2852

[35] Hoque M N F, Islam N, Li Z, Ren G F, Zhu K and Fan Z Y 2016 *Chemsuschem* **9** 2692

[36] Shi Z M, Cao Z, Sun X J, Jia Y P, Li D B, Cavallo L and Schwingenschlogl U 2019 *Small* **15** 1900462

[37] Mao L L, Guo P J, Kepenekian M, Spanopoulos I, He Y H, Katan C, Even J, Schaller R D, Seshadri R, Stoumpos C C and Kanatzidis M G 2020 *J. Am. Chem. Soc.* **142** 8342

[38] Lu D, Lv G W, Xu Z Y, Dong Y X, Ji X F and Liu Y S 2020 *J. Am. Chem. Soc.* **142** 11114

[39] Qu Z H, Ma F, Zhao Y, Chu X B, Yu S Q and You J B 2021 *Chin. Phys. Lett.* **38** 107801

[40] Dai Q X, Luo C, Wang X J, Gao F, Jiang X L and Zhao Q 2022 *Chin. Phys. B* **31** 037303

[41] Ahmad S, Fu P, Yu S W, Yang Q, Liu X, Wang X C, Wang X L, Guo X and Li C 2019 *Joule* **3** 794

[42] Quan L N, Yuan M J, Comin R, Voznyy O, Beauregard E M, Hoogland S, Buin A, Kirmani A R, Zhao K, Amassian A, Kim D H and Sargent E H 2016 *J. Am. Chem. Soc.* **138** 2649

[43] Stranks S D and Snaith H J 2015 *Nat. Nanotechnol.* **10** 391

[44] Tong C J, Geng W, Tang Z K, Yam C Y, Fan X L, Liu J, Lau W M and Liu L M 2015 *J. Phys. Chem. Lett.* **6** 3289

[45] Ma Z Q, Shao Y F, Wong P K, Shi X Q and Pan H 2018 *J. Phys. Chem. C* **122** 5844

[46] Ren H, Yu S D, Chao L F, Xia Y D, Sun Y H, Zuo S W, Li F, Niu T T, Yang Y G, Ju H X, Li B X, Du H Y, Gao X Y, Zhang J, Wang J P, Zhang L J, Chen Y H and Huang W 2020 *Nat. Photon.* **14** 154

[47] Xu Z Y, Lu D, Liu F, Lai H T, Wan X J, Zhang X D, Liu Y S and Chen Y S 2020 *Acs Nano* **14** 4871

[48] Yuan Y B and Huang J S 2016 *Acc. Chem. Res.* **49** 286

[49] Haruyama J, Sodeyama K, Han L Y and Tateyama Y 2015 *J. Am. Chem. Soc.* **137** 10048

[50] Yang J H, Yin W J, Park J S and Wei S H 2016 *J. Mater. Chem. A* **4** 13105

[51] Yang D W, Ming W M, Shi H L, Zhang L J and Du M H 2016 *Chem. Mater.* **28** 4349

[52] Knop O, Wasylishen R E, White M A, Cameron T S and Van Oort M J M 1990 *Can. J. Chem.* **68** 412

[53] Lee H, Gaiaschi S, Chapon P, Tondelier D, Bouree J E, Bonnassieux Y, Derycke V and Geffroy B 2019 *J. Phys. Chem. C* **123** 17728

[54] Lin Y, Bai Y, Fang Y J, Wang Q, Deng Y H and Huang J S 2017 *Acs Energy Lett.* **2** 1571

[55] Xiao X, Dai J, Fang Y J, Zhao J J, Zheng X P, Tang S, Rudd P N, Zeng X C and Huang J S 2018 *Acs Energy Lett.* **3** 684

[56] Mizusaki J, Arai K and Fueki K 1983 *Solid State Ionics* **11** 203

[57] Dualeh A, Moehl T, Tetreault N, Teuscher J, Gao P, Nazeeruddin M K and Gratzel M 2014 *Acs Nano* **8** 362

[58] Yang T Y, Gregori G, Pellet N, Gratzel M and Maier J 2015 *Angew. Chem. Int. Ed.* **54** 7905

[59] Yuan Y B, Wang Q, Shao Y C, Lu H D, Li T, Gruverman A and Huang J S 2016 *Adv. Energy Mater.* **6** 1501803

[60] Huang Z R, Proppe A H, Tan H R, Saidaminov M I, Tan F R, Mei A Y, Tan C S, Wei M Y, Hou Y, Han H W, Keley S O and Sargenet E H 2019 *Acs Energy Lett.* **4** 1521

[61] Lee H, Gaiaschi S, Chapon P, Marronnier A, Lee H, Vanel J C, Tondelier D, Bouree J E, Bonnassieux Y and Geffroy B 2017 *Acs Energy Lett.* **2** 943

[62] Cho J, DuBose J T, Le A N T and Kamat P V 2020 *ACS Materials Lett.* **2** 565

[63] Yuan Y B, Chae J, Shao Y C, Wang Q, Xiao Z G, Centrone A and Huang J S 2015 *Adv. Energy Mater.* **5** 1500615

[64] Zhang L, Liu Y C, Yang Z and Li S Z 2019 *J. Energy Chem.* **37** 97

[65] Kim S, Eom T, Ha Y S, Hong K H and Kim H 2020 *Chem. Mater.* **32** 4265

[66] Lee J W, Kim D H, Kim H S, Seo S W, Cho S M and Park N G 2015 *Adv. Energy Mater.* **5** 1501310

[67] Jeon N J, Noh J H, Yang W S, Kim Y C, Ryu S, Seo J and Seok S I 2015 *Nature* **517** 476

[68] Saliba M, Matsui T, Seo J Y, Domanski K, Correa-Baena J P, Nazeeruddin M K, Zakeeruddin S M, Tress W, Abate A, Hagfeldt A and Gratzel M 2016 *Energy Environ. sci.* **9** 1989

[69] Juarez-Perez E J, Ono L K, Maeda M, Jiang Y, Hawash Z and Qi Y B 2018 *J. Mater. Chem. A* **6** 9604

[70] Conings B, Drijkoningen J, Gauquelin N, Babayigit A, D'Haen J, D'Olieslaeger L, Ethirajan A, Verbeeck J, Manca J, Mosconi E, De Angelis F and Boyen H G 2015 *Adv. Energy Mater.* **5** 1500477

[71] Wang Y B, Wu T H, Barbaud J, Kong W Y, Cui D Y, Chen H, Yang X D and Han L Y 2019 *Science* **365** 687

[72] Juarez-Perez E J, Hawash Z, Raga S R, Ono L K and Qi Y B 2016 *Energy Environ. sci.* **9** 3406

[73] Wang S H, Jiang Y, Juarez-Perez E J, Ono L K and Qi Y B 2017 *Nat. Energy* **2** 16195

[74] Zhao Y X and Zhu K 2016 *Chem. Soc. Rev.* **45** 655

[75] Wu Y Z, Xie F X, Chen H, Yang X D, Su H M, Cai M L, Zhou Z M, Noda T and Han L Y 2017 *Adv. Mater.* **29** 1701073

[76] Di J, Chang J and Liu S 2020 *EcoMat* **2** e12036

[77] Wang Z P, Lin Q Q, Chmiel F P, Sakai N, Herz L M and Snaith H J 2017 *Nat. Energy* **2** 17135

[78] Park N G 2020 *Adv. Energy Mater.* **10** 1903106

[79] Dequilettes D W, Zhang W, Burlakov V M, Graham D J, Leijtens T, Osherov A, Bulovic V, Snaith H J, Ginger D S and Stranks S D 2016 *Nat. Commun.* **7** 11683

[80] Galisteo-Lopez J F, Li Y L and Miguez H 2016 *J. Phys. Chem. Lett.* **7** 5227

[81] Ma W F, Ding C J, Wazir N, Wang X S, Kong D N, Li A, Zou B S and Liu R B 2022 *Chin. Phys. B* **31** 037802

[82] Anaya M, Galisteo-Lopez J F, Calvo M E, Espinos J P and Miguez H 2018 *J. Phys. Chem. Lett.* **9** 3891

[83] Hoke E T, Slotcavage D J, Dohner E R, Bowring A R, Karunadasa H I and McGehee M D 2015 *Chem. Sci.* **6** 613

[84] Shah A, Torres P, Tscharner R, Wyrsch N and Keppner H 1999 *Science* **285** 692

[85] Fang H H, Yang J, Tao S X, Adjokatse S, Kamminga M E, Ye J T, Blake G R, Even J and Loi M A 2018 *Adv. Funct. Mater.* **28** 1800305

[86] Wu X X, Tan L Z, Shen X Z, Hu T, Miyata K, Trinh M T, Li R K, Coffee R, Liu S, Egger D A, Makasyuk I, Zheng Q, Fry A, Robinson J S, Smith M D, Guzelturk B, Karunadasa H I, Wang X J, Zhu X Y, Kronik L, Rappe A M and Lindenberg A M 2017 *Sci. Adv.* **3** e1602388

[87] Jiang X, Zang Z, Zhou Y, Li H, Wei Q and Ning Z 2021 *Acc. Mater. Res.* **2** 210

[88] Chen M, Dong Q S, Eickemeyer F T, Liu Y H, Dai Z H, Carl A D, Bahrami B, Chowdhury A H, Grimm R L, Shi Y T, Qiao Q Q, Zakeeruddin S M, Gratzel M and Padture N P 2020 *ACS Energy Lett.* **5** 2223

[89] Zhao J J, Deng Y H, Wei H T, Zheng X P, Yu Z H, Shao Y C, Shield J E and Huang J S 2017 *Sci. Adv.* **3** eaao5616

[90] Wu J H, Cui Y Q, Yu B C, Liu K, Li Y M, Li H S, Shi J J, Wu H J, Luo Y H, Li D M and Meng Q B 2019 *Adv. Funct. Mater.* **29** 1905336

[91] Xue D J, Hou Y, Liu S C, Wei M Y, Chen B, Huang Z R, Li Z B, Sun B, Proppe A H, Dong Y T, Saidaminov M I, Kelley S O, Hu J S and Sargent E H 2020 *Nat. Commun.* **11** 1514

[92] Feng G Q, Qin Y, Ran C, Ji L J, Dong L Y and Li W 2018 *APL Mater.* **6** 114201

[93] Wang H, Zhu C, Liu L, Ma S, Liu P F, Wu J F, Shi C B, Du Q, Hao Y M, Xiang S S, Chen H N, Chen P W, Bai Y, Zhou H P, Li Y J and Chen Q 2019 *Adv. Mater.* **31** 1904408